May 1985 LIDS-P-1461 NAG 2-297

MULTIVARIABLE CONTROL SYSTEMS WITH SATURATING ACTUATORS ANTIRESET WINDUP STRATEGIES*

by

Petros Kapasouris and Michael Athans

Laboratory for Information and Decision Systems
Massachusetts Institute of Technology
Cambridge, Massachusetts 02139

ABSTRACT

This paper contains preliminary; yet promising, results for introducing antireset windup (ARW) properties in multivariable feedback control systems with multiple saturating actuator nonlinearities and integrating action. The ARW method introduces simple nonlinear feedback around the integrators. The multiloop circle criterion is used to derive sufficient conditions for closed-loop stability that employ frequency-domain singular value tests. The improvement in transient response due to the ARW feedback is demonstrated using a 2-input 2-output control system based upon the F-404 jet engine dynamics.

1. Introduction

Reset-windups [1],[2] appear in feedback control when a linear compensator with integrators is used in a closed-loop system in the presence of saturating actuators. When the actuators are saturated the error is continuously integrated; this can lead to large overshoots on the response of the system. The antireset windup (ARW) idea is to use a linear compensator with a nonlinear feedback loop which "turns-off" the integrating action whenever saturation occurs. Then the large overshoots can be reduced and the performance of the system will improve (small overshoot, smaller settling times).

ARW techniques have been used extensively for single-input Single-output (SISO) systems [1,2]. The SISO ARW techniques are based on engineering intuition and on extensive simulations. Little mathematical analysis has been done even in the SISO case and we are not aware of any ARW strategies for MIMO systems. In this paper, we shall use the multivariable version of the circle criterion (see Safonov and Athans [3]) to develop sufficient conditions for the global stability of MIMO systems with saturation together with MIMO methods for ARW strategies. The theoretical examples are illustrated by a simple 2-input 2-output LQG/LTR based design [4],[5] using a model of the GE F-404 jet engine.

II. Mathematical Preliminaries

Assuming that all the signals belong in the extended L_2 space then a relation F is called stable in the extended L_2 space if there exists $K<\infty$ such that

$$||Fx|| \leq K||x|| \; ; \quad \forall x, \forall t \tag{1}$$

where

$$||x|| = \sqrt{<x,x>} \tag{2}$$

$$<x,x> \triangleq \int_0^t x_1^T(\tau)x_1(\tau)d\tau \tag{3}$$

The nonlinearities used in this paper are single-input single-output and time-invariant. We will say that a SISO mapping "f" is strictly inside a conic sector with radius r and center c if

$$\left|\frac{f(x)-cx}{x}\right|^2 < r^2-\varepsilon \qquad x\neq 0; \text{ for some } \varepsilon>0 \tag{4}$$

III. Statement of the Problem and Proposed Solution

Figure 1 shows a general MIMO closed loop system with several SISO saturating nonlinearities at the input of the plant. Except for the saturating nonlinearties the system is linear and time-invariant. A reasonable assumption is that the SISO actuator nonlinearities are memoryless (static) with upper and lower bounds U_i^H and U_i^L respectively. The input/output characterization of the nonlinearity f_i is given by

$$u_i^s(t) = \begin{cases} U_i^H & u_i(t) \geq U_i^H \\ u_i(t) & U_i^L \leq u_i(t) \leq U_i^H \\ U_i^L & u_i(t) \leq U_i^L \end{cases} \tag{5}$$

with i=1,2,....,p, where for p-control inputs

$$\underline{u}^s(t) \triangleq \begin{bmatrix} u_1^s(t) \\ \vdots \\ u_p^s(t) \end{bmatrix} \quad \underline{U}^H \triangleq \begin{bmatrix} U_1^H \\ \vdots \\ U_p^H \end{bmatrix} \quad \underline{U}^L \triangleq \begin{bmatrix} U_1^L \\ \vdots \\ U_p^L \end{bmatrix} \tag{6}$$

*Research supported by NASA Ames and Langley Research Centers under grant NASA/NAG 2-297 and by the General Electric Co.

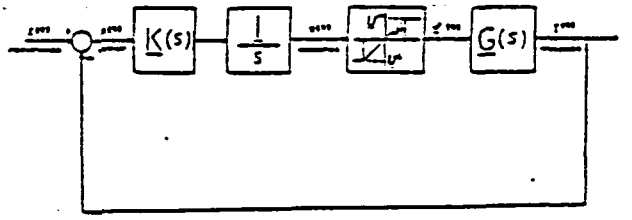

Figure 1: Closed loop MIMO system.

For a class of reference signals $\underline{r}(s)$ and initial conditions of $\underline{G}(s)$, the commanded control signal $\underline{u}(t)$ can exceed the saturation limits defined $\underline{U}^H$ and $\underline{U}^L$. Thus, "large" error signals are generated and are integrated continuously. The elements of the control vector $\underline{u}(t)$ does not necessarily change sign whenever those of the error vector $\underline{e}(t)$ do, because the integrator states can have large values at that time. Therefore one or more elements of the error vector $\underline{e}(t)$ may not be nulled-out for a substantial time before the correct component of changes sign, and this can lead to overshoots and large settling times in the transient responses.

Because the reset-windup problem is caused by the integrators it makes sense to "turn-off" the integrators whenever saturation occurs. Figure 2 shows a proposed nonlinear feedback system on the compensator $\underline{K}(s)$ and the integrators that will deactivate the integrators when such saturation occurs.

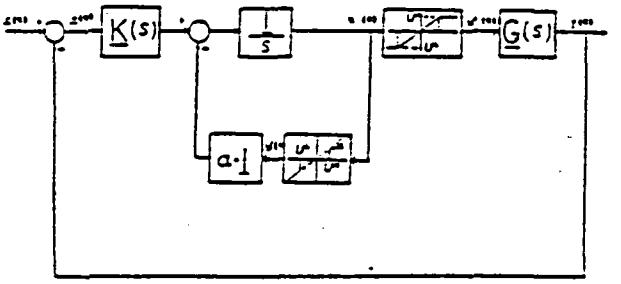

Figure 2: Closed-loop system with ARW properties.

The input/output characterization of the $\underline{f}_2$ nonlinearity, which consists of SISO "dead-zone" type elements, is given by

$$u_i^f(t) = \begin{cases} u_i(t) - U_i^H & u_i(t) \geq U_i^H \\ 0 & U_i^L \leq u_i(t) \leq U_i^H \\ u_i - U_i^L & u_i(t) \leq U_i^L \end{cases} \qquad (7)$$

where

$\underline{u}(t)$, $\underline{U}^H$ and $\underline{U}^L$ are defined in (6) and

$$u^f(t) = \begin{bmatrix} u_1^f(t) \\ \vdots \\ u_p^f(t) \end{bmatrix} \qquad (8)$$

From figure 2 it can be easily seen that when $\underline{u}(t)$ exceeds the saturation limits the following is true:

$$\underline{u}(s) = \frac{I}{s}\left[\underline{I} + \frac{I}{s}\alpha\right]^{-1}\underline{K}(s)\underline{e}(s) = \underline{K}(s)\,\frac{1}{s+\alpha}\,\underline{e}(s) \qquad (9)$$

Effectively the nonlinear feedback system replaces the integrators with a lag network. The design parameter α determines the time constant of the lag and it effects the stability of the closed-loop system. Section IV shows the stability analysis and how α can be determined.

IV. Stability Analysis

The closed-loop system in Figure 2 can be restructured to an equivalent one, as shown in Figure 3. Note the separation of the linear time invariant (LTI) part $\underline{T}(s)$ and the memoryless nonlinear time invariant part $\underline{F}$.

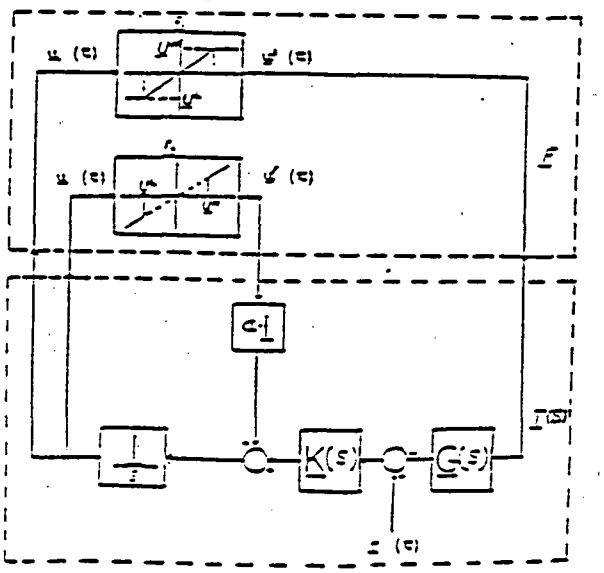

Figure 3: The closed loop system with ARW properties.

It is important to point out that since $\underline{K}(s)$, and $\underline{I}/s$ are linear systems the $\underline{r}(t)$ can enter at the $\underline{u}(t)$ signal as shown in Figure 4 without changing the stability of the closed loop system .

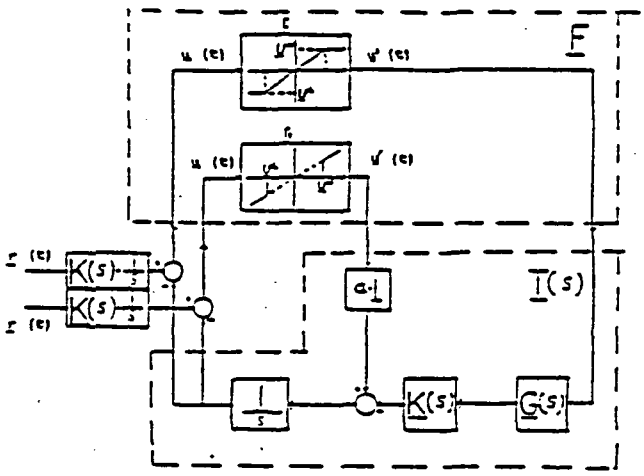

Figure 4: A system equivalent to that of Fig. 3.

Such modification is important in order to apply the multiloop circle criterion [3]. The mathematical equivalence of Figure 4 and Figure 3 can be easily seen by block diagram manipulation or by explicitly calculating the $\underline{y}(s)/\underline{u}(s)$ transfer functions for both configuration from Figures 3 or 4.

$$\underline{T}(s) = \begin{bmatrix} -\underline{K}(s)\underline{G}(s)\underline{I}/s & \frac{\alpha}{s}\underline{I} \\ -\underline{K}(s)\underline{G}(s)\underline{I}/s & \frac{\alpha}{s}\underline{I} \end{bmatrix} \tag{11}$$

$$\underline{u}^s(t) = \underline{f}_1(\underline{u}(t)) \tag{12}$$

$$\underline{u}^f(t) = \underline{f}_2(\underline{u}(t)) \tag{13}$$

$$\begin{bmatrix} \underline{u}^s(s) \\ \underline{u}^f(s) \end{bmatrix} = \underline{T}(s) \begin{bmatrix} \underline{u}(t) \\ \underline{u}(t) \end{bmatrix} \tag{14}$$

$$\underline{F} = \begin{bmatrix} \underline{f}_1 & 0 \\ 0 & \underline{f}_2 \end{bmatrix} \tag{15}$$

The $\underline{u}(t)$ signals (unsaturated controls) can be considered bounded (the bounds can be very large)

$$|u_i(t)| \leq U_i^M \quad \forall t; \quad -\infty < U_i^M < \infty; \quad \forall i \tag{16}$$

Then the $\underline{f}_1$ and $\underline{f}_2$ nonlinearities are strictly inside some conic sector as shown in Figures 5A and 5B.

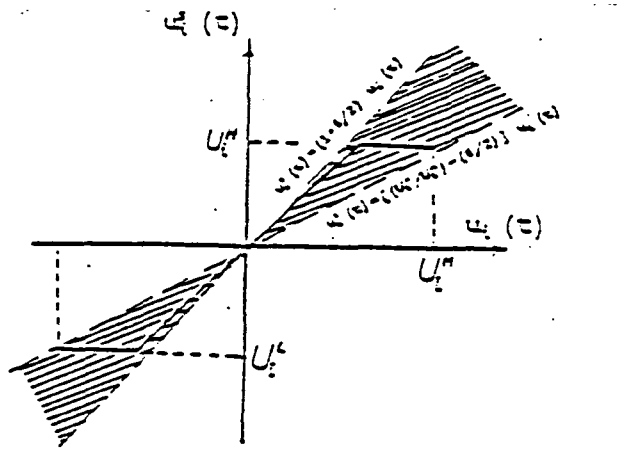

Figure 5a: Conic sector of the $\underline{f}_1$ nonlinearities.

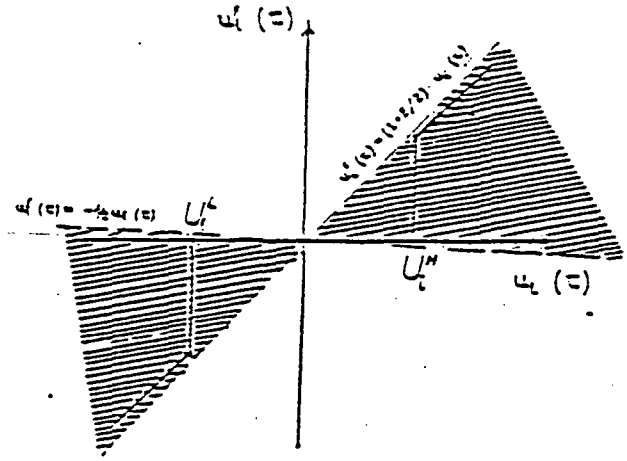

Figure 5b: Conic sector of the $\underline{f}_2$ nonlinearities.

The conic sector of the $\underline{f}_1$ nonlinearities, can be defined by a center C_i^1 and a radius r_i^1 where

$$C_i^1 + r_i^1 = 1+\varepsilon/2 \qquad \varepsilon>0;\ \varepsilon\to 0 \tag{17}$$

$$C_i^1 - r_i^1 = \frac{U_i^H}{U_i^H} - \varepsilon/2 \qquad \varepsilon>0;\ \varepsilon\to 0 \tag{18}$$

which implies that

$$r_i^1 = \left(1+\varepsilon - \frac{U_i^H}{U_i^M}\right)\cdot 1/2 \tag{19}$$

$$C_i^1 = 1+\varepsilon/2-r_i^1 \tag{20}$$

where

$$\underline{U}^H = \begin{bmatrix} U_1^H \\ \vdots \\ U_p^H \end{bmatrix} \quad \underline{U}^M = \begin{bmatrix} U_1^M \\ \vdots \\ U_p^M \end{bmatrix} \tag{21}$$

The U_i^H represents the high saturation limit in each input channel and it is a physical constraint. The U_i^M will be parameters in the stability analysis and they represent the worst bound on the unsaturated signals $U_i(t)$. $\underline{U}^M$ will be defined in the stability test to guarantee closed loop stability. Similarly a conic sector of each of the f_{i_2} nonlinearities can be defined by a center C_i^2 and radius r_i^2 as

$$C_i^2 = 1/2 \tag{22}$$

$$r_i^2 = 1/2 + \varepsilon/2 \qquad \varepsilon>0; \quad \varepsilon\sim 0 \tag{23}$$

define

$$\underline{C}^1 = \begin{bmatrix} C_1^1 & & 0 \\ & \ddots & \\ 0 & & C_p^1 \end{bmatrix}, \quad \underline{C}^2 = \begin{bmatrix} C_1^2 & & 0 \\ & \ddots & \\ 0 & & C_p^2 \end{bmatrix} \tag{24}$$

$$\underline{r}^1 = \begin{bmatrix} r_1^1 & & 0 \\ & \ddots & \\ 0 & & r_p^1 \end{bmatrix}, \quad \underline{r}^2 = \begin{bmatrix} r_1^2 & & 0 \\ & \ddots & \\ 0 & & r_p^2 \end{bmatrix} \tag{25}$$

$$\underline{C} = \begin{bmatrix} \underline{C}^1 & & 0 \\ & & \\ 0 & & \underline{C}^2 \end{bmatrix}, \quad \underline{R} = \begin{bmatrix} \underline{r}^1 & & 0 \\ & & \\ 0 & & \underline{r}^2 \end{bmatrix} \tag{26}$$

Stability Result

The multiloop circle criterion [3] can now be applied and sufficient conditions for stability are as follows:

1) The closed loop system has to be stable of the nonlinearities are replaced by their centers of their sectors $\underline{C}$.

2) The following has to be true for all frequencies

$$\sigma_{max}[\underline{R}\,\underline{T}(j\omega)[\underline{I}+\underline{C}\,\underline{T}(j\omega)]^{-1}] \leq 1 \quad \forall\omega \tag{27}$$

where $\underline{T}(s)$ has been defined by equation (11).

The only two parameters are α and $\underline{U}^M$, where α is the feedback loop gain parameter. Notice that different α's can be used for different directions on the feedback loop.

If for $\alpha=0$ the $\underline{U}^M$ given by the stability test is not satisfactory, the linear compensator design has to change or the specifications of the problem cannot be meet guaranting stability. In the multiloop circle criterion for $\alpha=0$ the AWR circuit is not used and the system is uneffected by the nonlinear ARW feedback.

A very important final point on the stability analysis is that the stability test is only a sufficient condition which means that if the conditions are satisfied then the closed loop system is guaranteed to remain stable. If the conditions are not satisfied then the closed loop system may or may not be closed loop stable, or the $\underline{U}^M$ is not a necessary bound for $\underline{u}(t)$.

V. Numerical Example

A linearized model of the GE F404 jet engine has been chosen corresponding to rated thrust condition at 35,000 ft altitude. The example is used here for academic purpose only. And the state-space representation of the scaled F-404 model is given by

$$\underline{\dot{x}}(t) = \begin{bmatrix} -1.46 & 2.35 & 0 \\ .321 & -2.23 & 0 \\ .175 & -.39 & 0 \end{bmatrix} \underline{x}(t) + \begin{bmatrix} .476 & 4.9 \\ .708 & .027 \\ .471 & -1.24 \end{bmatrix} \underline{u}(t)$$

$$\underline{y}(t) = \begin{bmatrix} 1 & 0 & 0 \\ 0 & 0 & 1 \end{bmatrix} \underline{x}(t) \tag{29}$$

$$\underline{G}(s) = \underline{C}(s\underline{I}-\underline{A})^{-1}\underline{B} \tag{30}$$

The components of the state vector $\underline{x}(t)$ are scaled and represent low pressure speed, high pressure speed, and thermocouple dynamics. The control vector components are

$u_1(t)$: scaled fuel flow with limits level
$-1\leq u_1(t)\leq 3$

$u_2(t)$: scaled nozzle area with limits
$-1\leq u_2(t)\leq +3$

The conic sectors that the input nonlinearities are strictly inside are given in figure 6. The conic sectors that the autowindup feedback nonlinearities are strictly inside are the same as always to the ones given in Section IV. With the given definition of the conic sectors the $\underline{C}$ and $\underline{R}$ matrices are

$$\underline{C} = \begin{bmatrix} 1/2(1-3/U_1^M) & & & 0 \\ & 1/2(1-3/U_2^M) & & \\ & & 1/2 & \\ 0 & & & 1/2 \end{bmatrix} \tag{31a}$$

$$\underline{R} = \begin{bmatrix} 1/2(1+\epsilon-3(U_1^M) & & 0 \\ & 1/2(1+\epsilon-3/U_2^M) & \\ & & 1/2+\epsilon/2 \\ 0 & & \\ & & 1/2+\epsilon/2 \end{bmatrix} \qquad (31b)$$

In the next step a compensator $\underline{K}(s)$ was designed using the LQG/LTR methodology [4,5] including an integrator on the Loop Transfer Matrix. The cross-over frequency region was set between approximately 4 and 10 rad/sec, the resultant singular values of the loop transfer matrix are shown in Figure 7. After the compensator was designed the following matrix was formed

$$\underline{T}(s) = \begin{bmatrix} -\underline{K}(s)\underline{G}(s)\frac{I}{s} & \frac{\alpha}{s}\underline{I} \\ -\underline{K}(s)\underline{G}(s)\frac{I}{s} & \frac{\alpha}{s}\underline{I} \end{bmatrix} \qquad (32)$$

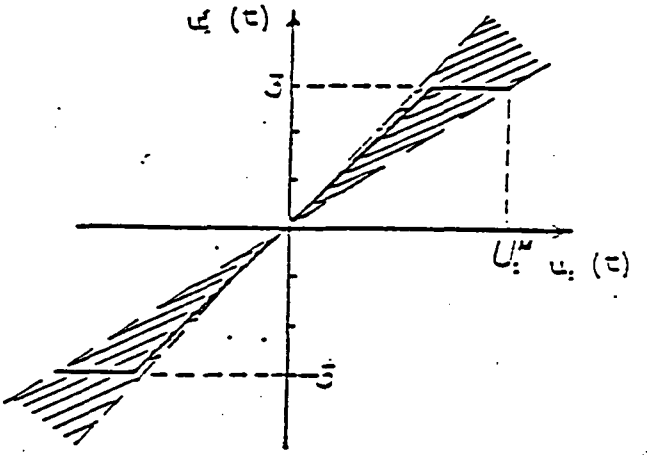

Figure 6a: Conic sector for the saturation of the fuel input of the F404 Engine.

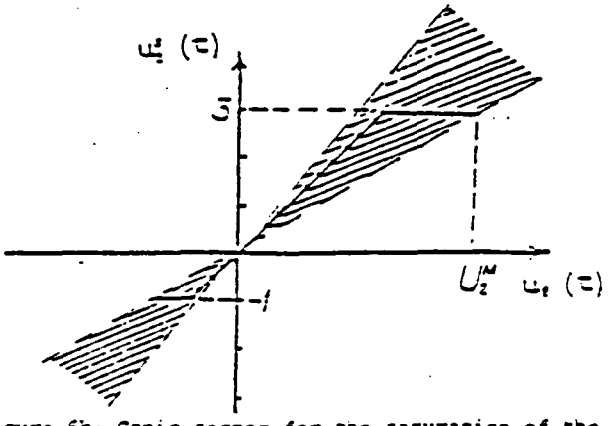

Figure 6b: Conic sector for the saturation of the nozzle input of the F404 Engine.

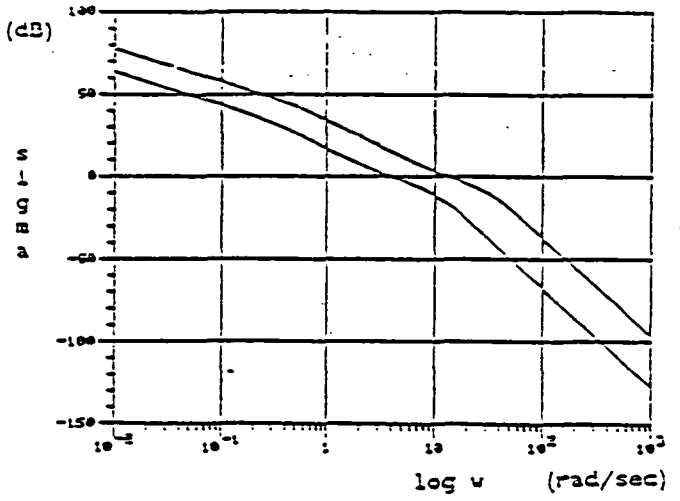

Figure 7: Singular values of the $\underline{G}(s)\underline{K}(s)\frac{I}{s}$.

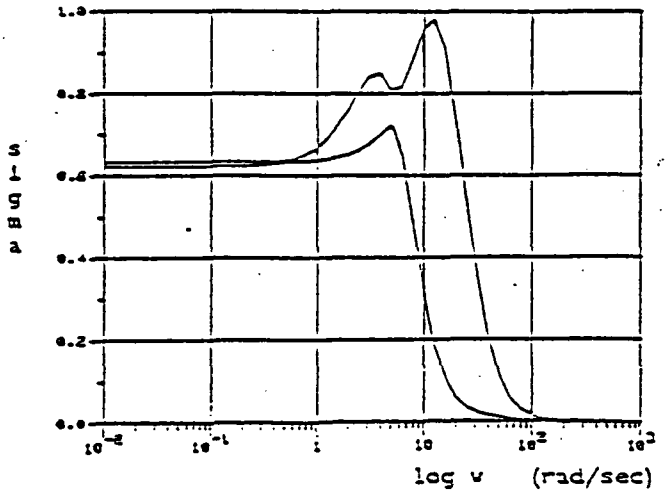

Figure 8: Singular value stability test (eq.33).

Recall that the test for closed loop stability was

$$\sigma_{max}[\underline{R}\,\underline{T}(j\omega)[\underline{I}+\underline{C}\,\underline{T}(j\omega)]^{-1}] \leq 1 \qquad \forall\omega \qquad (33)$$

It was found that for $\alpha=1$, $\epsilon/2=.0005$ and $\underline{U}_M=5\cdot\underline{I}$ the inequality (33) was satisfied for all frequencies as shown in Figure 8. Since the example is only for academic purposes the magnitude bound $\underline{U}_M$ for the $\underline{u}(t)$ signals will be considered sufficient. If the bound $\underline{U}_M$ is not sufficient not even for $\alpha=0$ then the compensator $\underline{K}(s)$ must be redesigned.

The second test for stability was to replace the nonlinearities with their centers $\underline{C}_i$, so for $\underline{U}^M = 5\cdot\underline{I}$

$$C = \begin{bmatrix} .8 & 0 \\ & .8 \\ & .5 \\ 0 & .5 \end{bmatrix} \qquad (34)$$

replacing the nonlinearities with C the closed loop system was find to be stable.

Since stability is guaranteed at least for $\underline{U}^M = 5 \cdot \underline{I}$. A simulation was performed with initial conditions $\underline{x}(0)$, constant reference signal $\underline{r}(t)$ and constant output disturbances $\underline{d}(t)$

$$\underline{x}(0) = \begin{bmatrix} -3 \\ -3 \\ -3 \end{bmatrix} \quad \underline{r}(t) = \begin{bmatrix} 2 \\ 1 \end{bmatrix}_{t \geq 0} \quad \underline{d}(t) = \begin{bmatrix} -.5 \\ -.5 \end{bmatrix}_{t \geq 0} \qquad (35)$$

Figure 9 shows the time responses of the closed loop system with and without ARW properties. One can readily see the performance improvement of the system with the ARW feedback.

Figure 10 shows the transient response of the saturated control input $u_s(t)$. Notice that the system with the ARW properties "takes action" faster than the original closed loop systems.

V. Conclusions

In this paper we have presented a promising technique for introducing antireset windup (ARW) properties in a linear MIMO control system with integrators which are followed by saturating nonlinearities. The design of the ARW feedback loops must be done in such a way so as to guarantee the stability of the nonlinear control system. We have explored the use of the multiloop circle to guide us in the ARW design.

We view the results in this paper as promising but certainly not complete. Much more research is needed to arrive at a generic design methodology to introduce ARW properties in a MIMO control system with multiple saturation nonlinearities. In particular, we plan to examine the degree of conservatism induced by the sufficiency conditions inherent in the use of the multiloop circle criterion, and means by which the conservatism can be decreased.

References

[1] A.H. Glattfelder and W.Schaufelberger, "Stability analysis of single loop control systems with saturation and antireset-windup circuits," IEEE Trans. on Auto. Control, Vol. AC-28, No. 12, December 1983.

[2] R. Hanns, "A new technique for preventing windup nuisances," Proc. IFIP Conf. on Auto. for Safety in Shipping and Offshore Petrol. Operations, 1980, pp. 221-224.

[3] M. Safonov and M. Athans, "A Multiloop generalization of the circle criterion for stability margin analysis," IEEE Trans. on Auto. Control, Vol. AC-26, No. 2, April 1981.

[4] J.C. Doyle and G. Stein, "Multivariable Feedback design: Concepts for a Classical/modern synthesis," IEEE Trans. on Auto. Control, Feb. 1981.

[5] G. Stein and M. Athans, "The LQG/LTR procedure for multivariable feedback control design," LIDS-P-1384, MIT, May 1984.

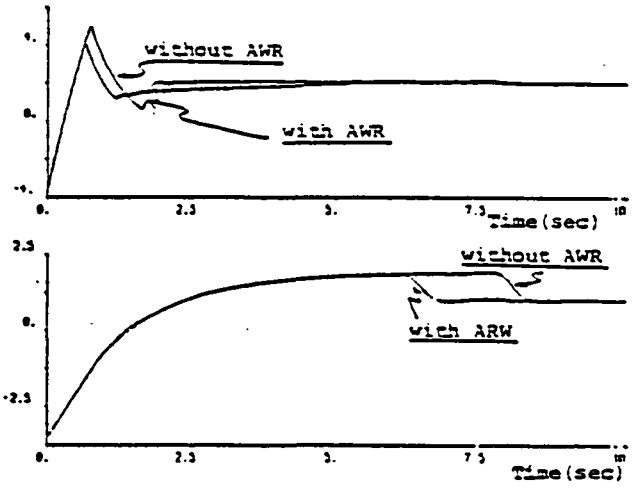

Figure 9: The output for both the original system and the one with AWR feedback. The top figure shows scaled low pressure speed transient and the bottom figure shows scaled temperature transient.

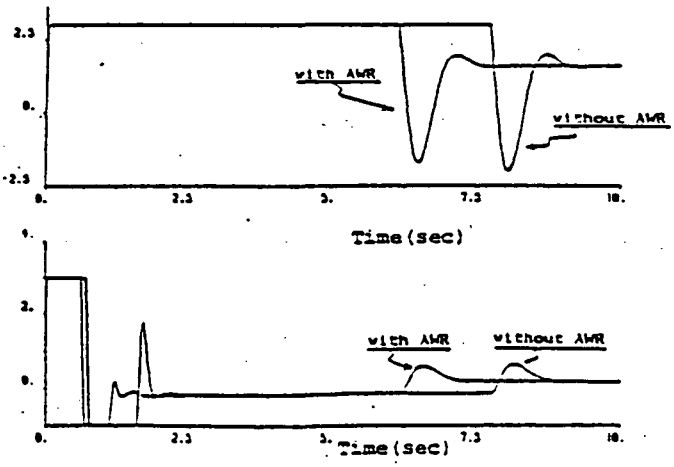

Figure 10: Saturated control inputs for both the original closed loop system and the one with feedback. The top figure shows the fuel flow response and the bottom one shows the nozzle area response.